Influence of Thermal Plasma Flow on the Mid-Latitude Nighttime F_2 Layer: Effects of Electric Fields and Neutral Winds Inside the Plasmasphere

C. G. PARK

Radioscience Laboratory, Stanford University, Stanford, California 94305

P. M. BANKS

Department of Applied Physics and Information Science
University of California at San Diego, La Jolla, California 92037

Theoretical models of the coupled ionosphere-plasmasphere system have been investigated with respect to processes occurring in the nighttime F_2 layer. It is found that plasma flow from the plasmasphere into the ionosphere has a strong stabilizing influence upon the peak F_2 region ion density N_mF_2 such that for wide ranges of applied east-west electric fields or north-south thermospheric winds there is essentially no change in the maximum density of the F_2 layer (N_mF_2). It is also found that N_mF_2 depends sensitively upon the plasma density of the plasmasphere and upon the neutral hydrogen concentration in the thermosphere. Time-dependent processes have been studied also by using step function electric fields and neutral winds. In the electric field case, squeezing of thermal plasma out of the plasmasphere along a contracting field tube significantly affects N_mF_2. Neutral thermospheric winds, on the other hand, have little effect on nighttime N_mF_2.

Many previous studies have emphasized the importance of thermal plasma flow between the ionosphere and the magnetosphere with regard to the characteristics of the F_2 region [e.g., *Hanson and Patterson,* 1964; *Yonezawa,* 1965; *Geisler and Bowhill,* 1965; *Stubbe,* 1968; *Nagy et al.,* 1968; *Park,* 1970; *Evans,* 1971; *Carpenter and Bowhill,* 1971; *Mayr et al.,* 1973; *Moffett and Murphy,* 1973]. At mid-latitudes inside the plasmasphere the problems surrounding the nighttime F_2 region have received special attention in efforts to isolate the basic processes that permit substantial ionization to exist in the presence of ionic recombination. Theoretical studies, however [*Stubbe,* 1968; *Kohl et al.,* 1969; *Stubbe and Chandra,* 1970; *Torr and Torr,* 1970; *Cho and Yeh,* 1970; *Rüster,* 1971], indicate that no one process is predominant with plasma flow from the high-altitude plasmasphere, vertical movements of ionization (from electric fields and neutral winds), corpuscular ionization, and perhaps even changes in atmospheric composition being of about equal importance.

In this paper we wish to present results of further theoretical work aimed at clarifying the effects of thermal plasma flow from the plasmasphere upon nighttime F_2 region densities. To do this, the continuity and momentum equations for O^+ and H^+ have been solved for a mid-latitude, closed field line geometry for which the regions above 3000 km are assumed to act as a finite volume thermal plasma reservoir. Solutions for time-varying and steady state east-west electric fields and meridional neutral winds have been obtained that give new information about the relative insensitivity of the F_2 layer peak density to changes in these parameters. It is also found that a close relation exists between the F_2 peak density, the H^+ density in the overlying plasmasphere and indirectly, the abundance of neutral atomic hydrogen. These relations are shown to arise as a consequence of thermal plasma flow induced by the balance of plasma pressure in the F_2 layer and the overlying plasmasphere.

The next section of this paper presents the theoretical concepts necessary for the present study. Then results for various conditions are given, and further discussion and conclusions follow.

THEORY

Our objective is to study the distribution of nighttime ion and electron density along geomagnetic field tubes between 150-km altitude and the geomagnetic equator with particular emphasis upon the F_2 region. The schematic diagram given in Figure 1 emphasizes the importance of thermal plasma flow from the high-altitude plasmasphere, which acts as a finite volume reservoir of thermal plasma in the form of H^+. Under proper conditions this plasma flows into the nighttime F_2 region, subject to the constraints of H^+/O^+ charge exchange, collisional friction, pressure gradients, gravity, and so forth. When meridional neutral winds are present in the F_2 region, we assume that the flux tube under consideration remains fixed in the rotating frame of the earth. For the east-west component of the electric field, however, there is a poleward or equatorward drift of the flux tube with an associated change in flux tube volume that induces a significant flow of plasma along the flux tube.

For the present model we divide our mid-latitude magnetic flux tube into three sections in which different simplifying assumptions can be made. Figure 2 illustrates these divisions with a flux tube having a unit cross-sectional area at 500-km altitude. Below 3000 km the geomagnetic field lines are assumed to be straight (this assumption introduces negligible errors at mid-latitudes). Above 3000 km a dipole field is assumed.

In region 1 ($150 < z < 500$ km) we assume that O^+ is the only ion present. Although molecular ions could have been included near the lower boundary, for the present problem of the nighttime F_2 layer their influence is entirely minimal. Near the upper boundary, H^+ is present in small amounts, but its effect upon the total electron density is negligible [e.g., *Banks and Kockarts,* 1973, chapter 21].

In region 2 ($500 < z < 3000$ km) a mixture of H^+ and O^+ is assumed, and the equations of continuity and momentum

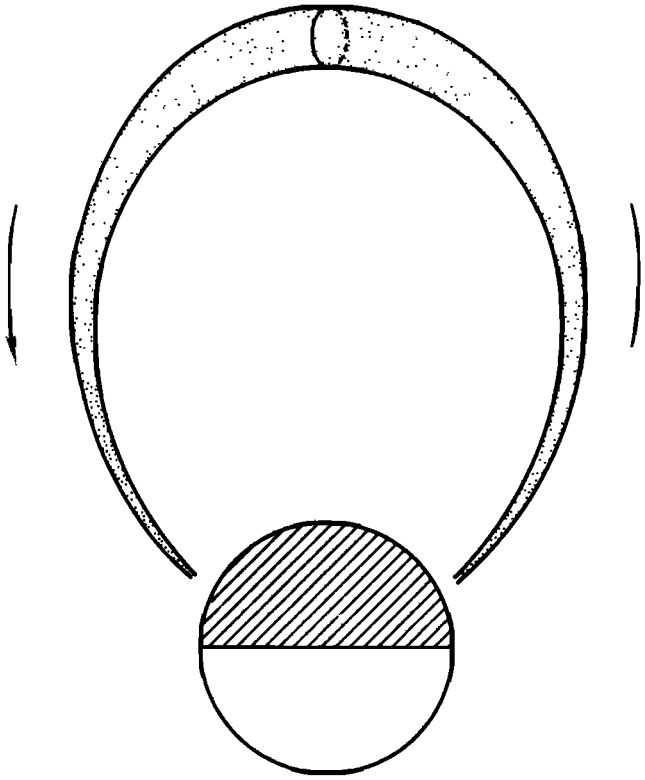

Fig. 1. Illustration of the general idea of ionosphere-plasmasphere (plasma) coupling; H^+ stored along a field tube in the outer plasmasphere is free to flow into the nighttime F_2 region to maintain a significant ion density in regions of appreciable ionization loss.

must take into account the resulting nonlinearities that govern the individual ion densities and flow speed. The presence of He^+ is neglected on the basis of ion mass spectrometer results for the midgeomagnetic latitude regions [e.g., *Taylor et al.*, 1968].

In region 3 ($z > 3000$ km), H^+ is assumed to be the dominant ion acting under the influence of gravity, plasma pressure gradients, and imposed external electric fields.

The basic equations describing the plasma density and flow for the three regions described above are given below.

Region 1 (150 < z < 500 km). The basic equation of continuity for O^+ is

$$\frac{\partial n(O^+)}{\partial t} + \frac{1}{A}\frac{\partial [n(O^+) w A]}{\partial z} = p - \beta n(O^+) \qquad (1)$$

where $n(O^+)$ is the O^+ density, p is the O^+ production rate, A is the area of the flux tube, w is the O^+ vertical transport speed, z is a vertical coordinate, and β is the O^+ ionization loss rate.

For our nighttime models the production rate p is zero, but it will be retained in the following equations for completeness. The ion loss coefficient β is approximated by

$$\beta = \frac{1.1 \times 10^{-9}}{T_i^{0.7}} n(O_2) + \left[12 - \frac{(T_n - 300)}{50} + \frac{(T_n - 300)(T_n - 600)}{3.5 \times 10^4}\right] \times 10^{-13} n(N_2) \quad s^{-1}$$

obtained from the data of *McFarland et al.* [1973] by using empirical curve fitting. In this expression the neutral gas temperature T_n is taken from models of the neutral atmosphere. The ion temperature T_i is computed from the electron temperature T_e, and T_n is described later.

The cross-sectional area of the plasma-filled flux tube sketched in Figure 2 is given by $A(z) = [(R_E + z)/(R_E + z_2)]^3$, where R_E is the earth radius and z_2 is the 500-km boundary altitude.

For the ion vertical velocity w we use the standard low-speed, time-independent form of the O^+ momentum equation, which separates contributions from diffusion and externally imposed drift:

$$w = -D\left\{\frac{\partial \ln n(O^+)}{\partial z} + \frac{\partial \ln T_p}{\partial z} + \frac{1}{H_p}\right\} + w_D \qquad (2)$$

where $T_p = T_e + T_i$ and $H_p = kT_p/m_i g$, m_i being the ion mass and g the acceleration of gravity.

The quantity D in (2) is an effective ambipolar diffusion coefficient that takes into account the effect of the magnetic field dip angle I; i.e., $D = (1 + T_e/T_i) \sin^2 I \, D_{in}$, where D_{in} is the diffusion coefficent of O^+ in the neutral atmosphere [*Banks and Kockarts*, 1973, chapter 19]:

$$D_{in}^{-1} = \frac{(1 + T_n/T_i)^{1/2}}{3.1 \times 10^{17} T_i^{1/2}} n(O) + \frac{1}{7.2 \times 10^{15} T_i} n(O_2) + \frac{1}{8.5 \times 10^{15} T_i} n(N_2) \quad s^2 \ cm^{-1} \qquad (3)$$

In the F_2 region the vertical drift velocity w_D, measured as being positive upward, is given by

$$w_D = -(cE_y/B) \cos I - U_x \sin I \cos I \qquad (4)$$

where E_y is the westward component of the electric field and U_x is the northward moving meridional wind. Zonal neutral winds and plasma drifts that result in Joule heating and other effects are not included in this study.

With the foregoing information the time-dependent con-

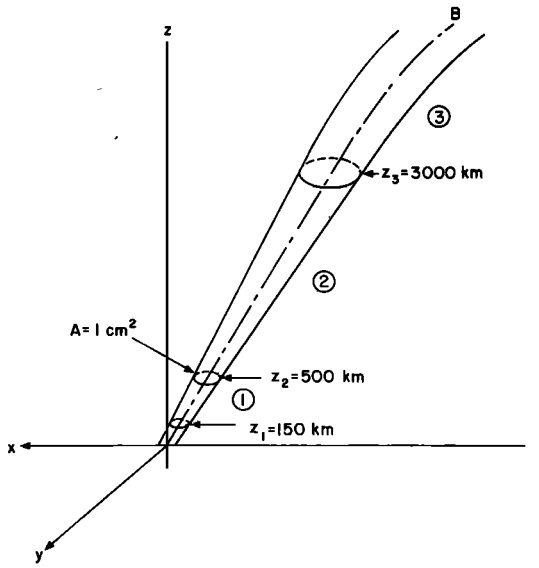

Fig. 2. The three separate regions discussed in the text are shown with the adopted coordinate system. The coordinate x points to the north, y to the west. The area of flux tube is measured orthogonally to **B**.

tinuity equation for O^+ can be rewritten as

$$\frac{1}{D}\frac{\partial n(O^+)}{\partial t} - \frac{\partial^2 n(O^+)}{\partial z^2} - a(z)\frac{\partial n(O^+)}{\partial z} - b(z)n(O^+) = p/D \quad (5)$$

where

$$a(z) = \frac{\partial}{\partial z}\ln(AT_pD) + \frac{1}{H_p} - \frac{w_D}{D}$$

$$b(z) = \left(\frac{\partial \ln T_p}{\partial z} + \frac{1}{H_p} - \frac{w_D}{D}\right)\frac{\partial \ln A}{\partial z} + \left(\frac{\partial \ln T_p}{\partial z} + \frac{1}{H_p}\right)\frac{\partial \ln D}{\partial z} + \frac{\partial^2 \ln T_p}{\partial z^2} + \frac{\partial}{\partial z}\frac{1}{H_p} - \frac{1}{D}\frac{\partial w_D}{\partial z} - \frac{\beta}{D}$$

Solutions to (5) can be obtained by using standard numerical techniques. To do so, however, requires that we impose physically meaningful boundary conditions. At the lower boundary of region 1 we would normally specify a condition of chemical equilibrium, i.e., $n = p/\beta$. Since, however, $p = 0$ at nighttime, an equivalent condition is $n_{150}(O^+) = 0$ at 150-km altitude. At the upper boundary of 500 km a flux condition is imposed to reflect the transfer of ionization from region 2 into region 1 (or vice versa). This condition is expressed as

$$\Phi_{500}(O^+) = \int_{500}^{3000}\left[p(H^+) - \beta(H^+)n(H^+) + \frac{\partial n(O^+)}{\partial t}\right]A(z)\,dz$$

where $\Phi(O^+) = n(O^+)wA$ and the value 500 refers to the 500-km boundary altitude separating regions 1 and 2. Also, $p(H^+)$ is the H^+ production rate, and $\beta(H^+)$ is the H^+ loss rate.

With regard to the thermal balance in region 1 we make no attempt to solve the complete electron energy balance equations for T_e and T_i. Instead, T_e is adopted from the experimental values obtained by *Evans* [1967] at mid-latitudes. The ion temperature is computed from the electron and neutral gas temperatures by using expressions developed previously [e.g., *Banks and Kockarts,* 1973, chapter 23].

Region 2 (500 < z < 3000 km). In this region a mixture of O^+ and H^+ is considered, and the transport processes affecting each ion species must be considered separately. For O^+ diffusion, friction at F_2 region heights and above is provided mainly by momentum transfer with atomic oxygen atoms. Above 500 km, however, $n(O)$ is sufficiently low that O^+-O friction is relatively unimportant in the O^+ momentum equation [e.g., *Banks and Holzer,* 1969]. In a similar manner the motion of H^+ ions is also unimpeded by the neutral atmosphere. Nevertheless, when there is a net relative flow of H^+ and O^+, the large momentum transfer cross section for coulomb collisions between the two ion gases insures that a substantial momentum transfer must take place, which is reflected in the consequent ion density distributions.

Following derivations given elsewhere [e.g., *Banks and Kockarts,* 1973], the momentum equation for O^+ can be written as

$$\frac{1}{n(O^+)}\frac{\partial n(O^+)}{\partial z} + \frac{T_e}{T_i}\frac{\partial \ln N_e}{\partial z} + \frac{\partial \ln T_i}{\partial z} + \frac{T_e}{T_i}\frac{\partial \ln T_e}{\partial z} = 0 \quad (6)$$

where $n(O^+)$ is the O^+ density, T_i is the ion temperature, N_e is the electron density, and the relatively minor effect of H^+-O^+ momentum transfer upon the O^+ distribution is omitted [*Banks and Kockarts,* 1973, chapter 21]. When the value $n_{500}(O^+)$ is specified, (6) can be solved in conjunction with a more complex equation describing H^+ to give self-consistent, time-dependent electron and ion density distributions between 500 and 3000 km.

With regard to H^+ the equation of continuity can be written as

$$\frac{\partial n(H^+)}{\partial t} + \frac{1}{A}\frac{\partial [n(H^+)w_1A]}{\partial z} = p_1 - \beta_1 n(H^+) \quad (7)$$

where w_1 is the H^+ vertical diffusion velocity.

The production and loss of H^+ takes place through the charge exchange reaction

$$O + H^+ \rightleftarrows O^+ + H$$

at the rates

$$p(H^+) = 2.5 \times 10^{-11} T_n^{1/2} n(O^+) n(H) \quad cm^{-3}\ s^{-1}$$

$$\beta(H^+) = 2.3 \times 10^{-11} T_i^{1/2} n(O) \quad s^{-1}$$

If the H^+ flow speed is slow in comparison with the H^+ thermal speed $(kT_i/m_1)^{1/2}$ the time-independent momentum equation for H^+ is

$$w_1 = -D_1\left[\frac{\partial \ln (n(H^+)T_i)}{\partial z} + \frac{T_e}{T_i}\frac{\partial \ln (N_eT_e)}{\partial z} + \frac{1}{H_1}\right] + w_D \quad (8)$$

where $H_1 = kT_i/m(H^+)$, T_i is the H^+ temperature, and w_D is the ion vertical drift speed given by (4). The diffusion coefficient D_1 is given by [*Schunk and Walker,* 1970]

$$D_1 = \frac{6.88 \times 10^7 T_i^{5/2}}{n(O^+)}\sin^2 I \quad cm^2\ s^{-1}$$

If (7) and (8) are used, the time-dependent equation describing the H^+ density in region 2 becomes

$$\frac{1}{D_1}\frac{\partial n(H^+)}{\partial t} - \frac{\partial^2 n(H^+)}{\partial z^2} - c(z)\frac{\partial n(H^+)}{\partial z} - d(z)\,n(H^+) = p(H^+)/D_1 \quad (9)$$

where

$$c(z) = \frac{T_e}{T_i}\frac{\partial}{\partial z}\ln(N_eT_e) + \frac{\partial}{\partial z}\ln(T_iD_1A) + \frac{1}{H_1} - \frac{w_D}{D_1}$$

$$d(z) = \frac{T_e}{T_i}\frac{\partial^2 \ln N_e}{\partial z^2} + \left[\frac{T_e}{T_i}\frac{\partial \ln (D_1 A)}{\partial z} + \frac{\partial}{\partial z}\frac{T_e}{T_i}\right]\frac{\partial \ln (N_e T_e)}{\partial z} + \frac{T_e}{T_i}\frac{\partial^2 \ln T_e}{\partial z^2} + \frac{\partial^2 \ln T_i}{\partial z^2} + \left[\frac{\partial \ln (D_1 A)}{\partial z}\right] \cdot \left[\frac{\partial \ln T_i}{\partial z} + \frac{1}{H_1}\right] + \frac{\partial}{\partial z}\frac{1}{H_1} - \frac{\beta(H^+)}{D_1} - \frac{w_D}{D_1}\frac{\partial \ln A}{\partial z} - \frac{1}{D_1}\frac{\partial w_D}{\partial z}$$

As occurs in region 1, time-dependent solutions for the O^+ and H^+ densities require appropriate boundary conditions. For H^+ we assume that chemical equilibrium prevails at 500 km, so that $n_{500}(H^+) = p(H^+)/\beta_{500}(H^+)$. At the upper boundary (3000 km) we specify a second H^+ density, $n_{3000}(H^+)$, which is obtained from the reservoir calculations of region 3. When $n_{500}(H^+)$, $n_{500}(O^+)$, and $n_{3000}(H^+)$ are specified, it is possible to solve (6) and (9) for the O^+ and H^+ density profiles once the profile of electron and ion temperature is given.

For the present study we adopt a simple profile of electron temperature above 500 km, using the assumption of a constant electron heat flow given by

$$F = -7.7 \times 10^5 T_e^{5/2} A(\partial T_e/\partial z) \quad \text{eV cm}^{-2}\,\text{s}^{-1}$$

where F is the electron heat flux across the 500-km level. In this expression, A is the magnetic field tube area given by (2), and the remaining part of the expression follows from the standard expression for a fully ionized gas. If F is assumed to be constant with altitude, the explicit electron temperature profile is

$$T_e(z) = \left\{T_e(z_1)^{7/2} + 2.28 \times 10^{-6} \cdot (R_E + z_2)\left[\left(\frac{R_E + z_2}{R_E + z}\right)^2 - 1\right]F\right\}^{2/7} \qquad (10)$$

The corresponding ion temperature profile is obtained by using the technique described for region 1 and ignoring ion thermal conduction.

Since (6) and (9) are coupled and nonlinear, numerical solutions are obtained by using linearized forms requiring iteration between successive time steps.

Region 3 ($z > 3000$ km). The distribution of H^+ along magnetic field lines depends strongly upon the thermal structure of this region. Owing to certain difficulties in our knowledge of the electron thermal conductivity in the plasmasphere [*Mayr et al.*, 1973], theoretical models of plasma temperatures in this region cannot be trusted, and as a consequence, we have made no attempt to derive ionization profiles. Instead, we use a simple reservoir idea that relies upon particle number conservation in the regions above 3000 km to determine the H^+ density at the 3000-km level. This last quantity is needed as a density boundary condition for the region 2 calculations.

Briefly, we assume initial values for the 3000-km H^+ density consistent with the total field tube plasma content N_T. This latter quantity is defined as the total number of H^+ ions in the flux tube lying between 3000-km altitude and the geomagnetic equator. Changes in N_T arise both from H^+ fluxes at 3000 km and from changes in field tube volume V_T arising from $\mathbf{E} \times \mathbf{B}$ drift. If we assume that the shape of the H^+ distribution along $\mathbf{B}$ remains the same for such changes in the field tube volume, then the H^+ density at 3000 km at any time is related to the total tube content and volume by the expression

$$n_{3000}(H^+) = n_{3000}^0(H^+)(N_T/N_T^0)(V_T^0/V_T) \qquad (11)$$

where the superscript 0 refers to the initial values at some time t_0.

RESULTS

Steady state solutions. The equations derived in the last section have been solved for steady state nighttime conditions using several models for the neutral atmosphere. In these particular calculations a flux tube ionization content of $N_T = 5 \times 10^{13}$ ions cm^{-2} has been chosen on the basis of mid-latitude whistler observations. The depletion of plasma in the flux tube reservoir above 3000 km has been neglected for this typical content, since the time needed to achieve a steady state is much smaller than the time needed to reduce appreciably the reservoir of plasma content (a flux of 5×10^8 ions cm^{-2} s^{-1} reduces N_T by 10% only after 4 hours). In the real case, prolonged downward flow of H^+ clearly depletes the reservoir and reduces the 3000-km H^+ density. However, for the present section we want to illustrate several interesting effects of this downward flow upon the F_2 region. Therefore we do not attempt to reproduce the complete sequence of a nocturnal decay of the coupled F_2 region and topside ionosphere.

The atmospheric models used in these calculations are taken from Appendix B of *Banks and Kockarts* [1973]. Models M750, M1000, and M1250, representing thermopause temperatures of 750°, 1000°, and 1250°K, respectively, are taken directly from the published tables, whereas M*750 and M*1250 have atomic hydrogen densities corresponding to the atomic hydrogen density of M1000. As a consequence, the atomic hydrogen density for M*750 is smaller than that for M750, whereas the opposite is true for M*1250 and M1250.

Figure 3 illustrates the results for the steady state solutions at 50° geomagnetic latitude, using M1000 and electron temperature data for November 1964 [*Evans*, 1967]. Solutions for region 1 provide the solid curves showing the relationship between the O^+ fluxes across the 500-km level and $n(O^+)$ at 500

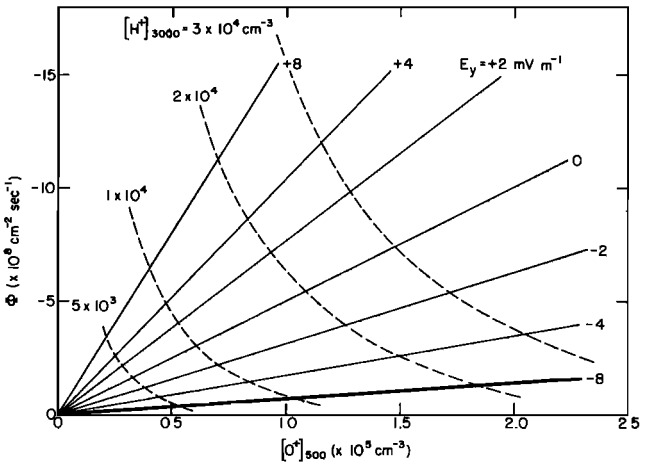

Fig. 3. Results for steady state conditions in regions 1 and 2. The solid lines give values of the 500-km O^+ density as a function of the 500-km O^+ flux for seven values of E_y. The dashed curves give values of the H^+ flux at 3000 km (normalized to 500 km) for four values of the 3000-km H^+ density.

km. A positive value of the electric field is directed westward and causes a downward drift of F_2 region ionization. In region 2, H^+ and O^+ profiles are computed for different values of the boundary ion densities at 500 km and 3000 km. The four dashed curves in Figure 3 show the quantity $\Phi(H^+)$ (note that $\Phi(H^+) = n(H^+)w_1A$) at 3000 km for four values of $n_{3000}(H^+)$. In a steady state the flow of H^+ across the 3000-km level must equal the flow of O^+ across the 500-km level. Therefore each intersection between a solid and a dashed curve represents a steady state solution. Thus, for example, if $E_y = 0$, decreases in the H^+ density at 3000 km lead to corresponding decreases in the 500-km O^+ density. To illustrate the vertical profiles of ion composition, Figure 4*a* shows $n(O^+)$, $n(H^+)$ for $E_y = -6$ mV m^{-1} and $n_{3000}(H^+) = 10^4$ cm^{-3}. Figure 4*b* shows the corresponding temperature profiles.

Returning to Figure 3, we can deduce several important properties of the coupled ionosphere-plasmasphere system. For a given E_y, $n_{500}(O^+)$ increases almost linearly with $n_{3000}(H^+)$. Since the height distribution of O^+ below 500 km remains unchanged in shape (in a purely accretive layer with zero production the height of the F_2 layer peak density h_mF_2 does not depend upon the magnitude of the flux), it follows that N_mF_2 is directly proportional to the plasmasphere density at 3000 km.

Now consider a case in which the 3000-km density is fixed by conditions of the plasmasphere reservoir but E_y changes. From Figure 3 we see that when E_y increases (becomes more positive in the westward sense), a larger downward flow of O^+ across the 500-km level is required to compensate for increased ion losses as the F_2 layer is pushed deeper into the atmosphere. This variation is illustrated also in Figure 5 from a slightly different point of view. If the flux across the 500-km level is fixed at -10^8 cm^{-2} s^{-1}, N_mF_2 (lower horizontal scale) varies with E_y, as is shown by the dashed curve. The actual flux across the 500-km level for $n_{3000}(H^+) = 10^4$ cm^{-3} is shown by the dash-dot line (upper scale) as a function of E_y. The product of these two curves gives N_mF_2 shown as the solid curve. A remarkable result of the ionosphere-plasmasphere coupling process is at once evident: for a wide range of O^+ vertical drift velocities the peak density of the F_2 layer is fixed in magnitude, greater F_2 region ion losses being compensated by a proportionately larger downward flux of H^+ from the plasmasphere.

Although this constancy of N_mF_2 has been described above in terms of the westward component of the electric field, meridional neutral winds may yield similar results, as is indicated by the scales on the left side of Figure 5. At night, for example, neutral winds of -100 to -200 m s^{-1} place N_mF_2 in the vertical part of the computed curve, where changes in neutral wind (or electric field) give negligible changes in F_2 region peak density.

Although the maximum F_2 layer density is relatively insensitive to changes in E_y or U_x, the height of the peak does change, as is shown in Figure 6 for three models of the neutral atmosphere.

Figure 7 illustrates the ionospheric effects of changing ionization loss coefficients. The solid curve is reproduced from Figure 5 and serves as a reference point for the subsequent changes. The dashed curve results from reducing the O^+ loss coefficient by a factor of 2. The broken curve follows when $n(O)$ is increased at all altitudes by a factor of 2, this increase thereby reducing the O^+ diffusion coefficient. It can be seen that these changes have a surprisingly small effect upon the F_2 layer peak density.

The results of calculations similar to the foregoing are shown for different models of the neutral atmosphere in Figure 8, where N_mF_2 is given as a function of westward electric field E_y. The solid curve, reproduced from Figure 5, gives the result obtained for a 1000°K model atmosphere. For all the models, N_mF_2 is nearly independent of E_y for $E_y \lesssim -2$ mV m^{-1} or equivalently, for $U_x \lesssim -50$ m s^{-1}. When the external drift velocity imposed upon the F_2 layer becomes too large, however, the F_2 layer is pushed deep within the atmosphere, and ion losses become so great that matching downward fluxes from the plasmasphere can no longer be drawn. In this situation, N_mF_2 rapidly begins to decrease with increasing downward drift velocity.

It has also been found that the differences in N_mF_2 for the different models of the neutral atmosphere are mainly a result of changes in the neutral hydrogen densities with consequent effect upon $n(H^+)$. When $n(H)$ decreases, as it does in going from M750 to M*750, $n_{500}(H^+)$ decreases, its decrease giving for a fixed value of $n_{3000}(H^+)$ a larger downward flux from the

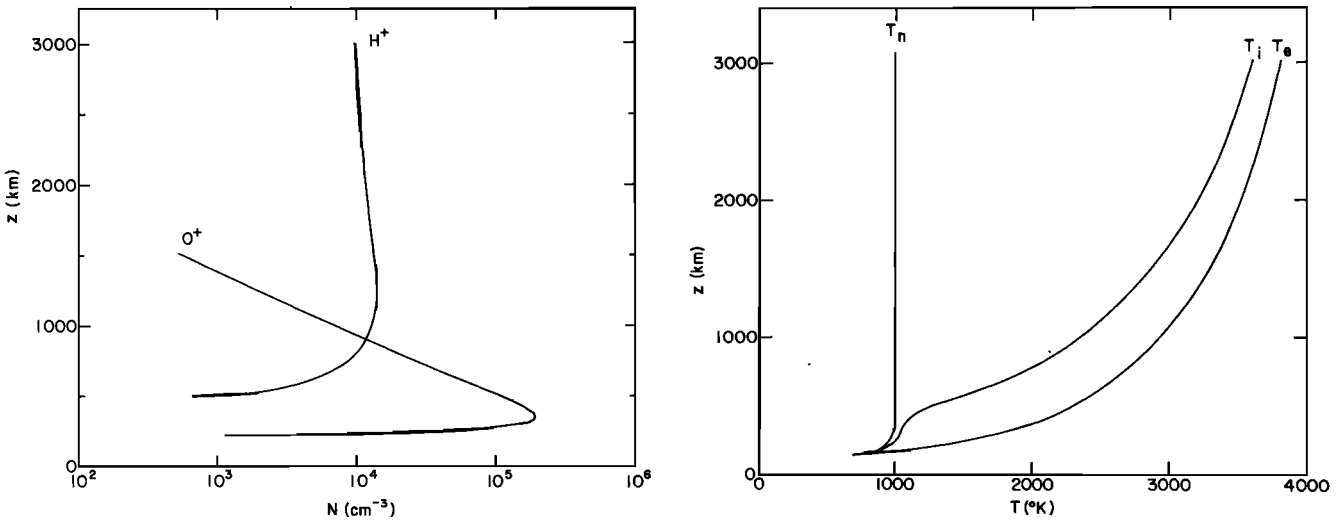

Fig. 4. (*a*) Examples of the steady state vertical profiles of ion composition for $E_y = -6$ mV m^{-1} and $n_{3000}(H^+) = 10^4$ cm^{-3}. (*b*) Plasma temperature profiles used in computing Figure 4*a*. An electron heat flux of 5×10^9 eV cm^{-2} s^{-1} has been assumed above 500 km.

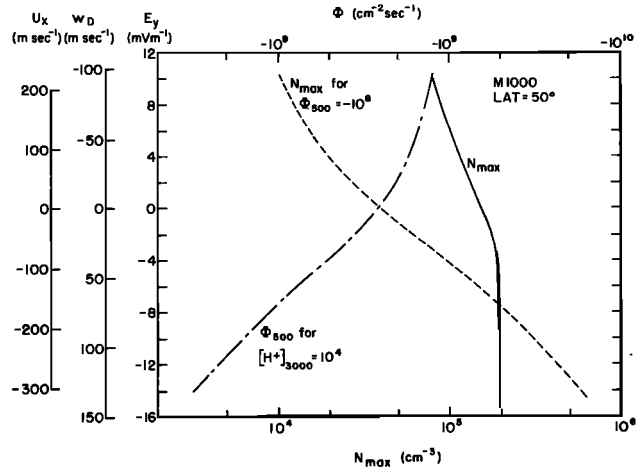

Fig. 5. Variation of N_mF_2 and Φ_{500} for different vertical drift velocities with atmospheric model M1000 at 50° geomagnetic latitude.

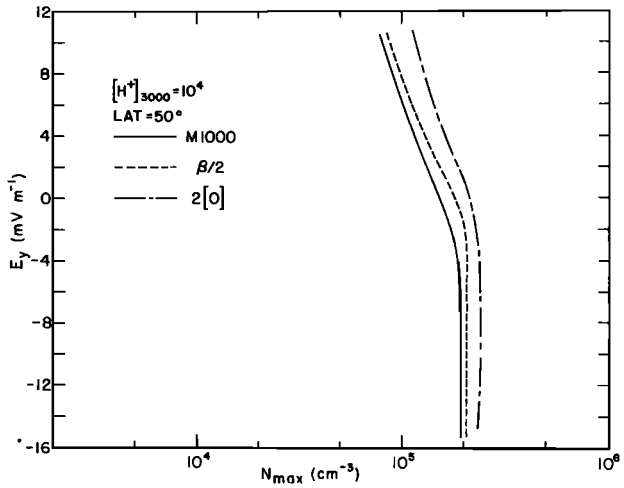

Fig. 7. Peak F_2 layer density as a function of E_y for changes in the ionization loss rate and O^+ diffusion coefficient. The solid line gives the previous result for a 1000°K thermosphere.

plasmasphere and a larger value of N_mF_2. Since large changes occur in neutral hydrogen concentrations in the course of a solar cycle, these results imply a solar cycle dependence in the behavior of the nighttime F_2 region.

As a consequence of the foregoing results, we deduce that the thermal plasma of the plasmasphere exerts a strong control over the peak electron density in the nighttime ionosphere by adjusting the downward fluxes to compensate for changes in rate coefficients or vertical movements of the layer. Thus in computations of the effects of winds or electric fields upon the nighttime F_2 layer it is not sufficient to assume that O^+ is in diffusive equilibrium at some upper boundary: the absence of significant O^+-O friction in the regions above the F_2 peak density allows large downward O^+ fluxes to be present while it gives an O^+ density profile that is indistinguishable from the zero flow diffusive equilibrium case. The magnitude of the downward flow, however, can be obtained only by considering the coupled ionosphere-plasmasphere system including the behavior of O^+ and H^+.

Time-dependent solutions. For this part of the study we begin with steady state density distribution solutions obtained in the manner described above and then subject the ionosphere-plasmasphere system to a sudden change in meridional neutral wind or westward electric field. As is described above, in the steady state models, in which the plasma density at 3000 km is held fixed, neutral winds and electric fields have identical effects below 3000 km as long as they induce the same vertical drift velocity. For the time-dependent electric field case, in contrast, the plasmaspheric density at 3000 km changes with time owing to changes in field tube volume and the overall plasma content. With neutral winds, however, the field tube volume remains constant as the plasma content changes. As a consequence, electric fields and neutral winds can be expected to have different effects upon the F_2 region when they undergo sudden changes.

Figure 9 shows a plot of magnetic field tube volume as a function of L shell [*Park*, 1972]. If an east-west electric field is applied, the tube volume can be computed as a function of time from the equatorward drift velocity $(\mathbf{E} \times \mathbf{B})/B^2$. The corresponding changes in $n_{3000}(H^+)$ follow directly from (11).

Figure 10 shows an example for the response of the F_2 region to sudden changes in E_y and U_x. In Figure 10*a* a westward electric field is applied at time $t = 0$, and in Figure

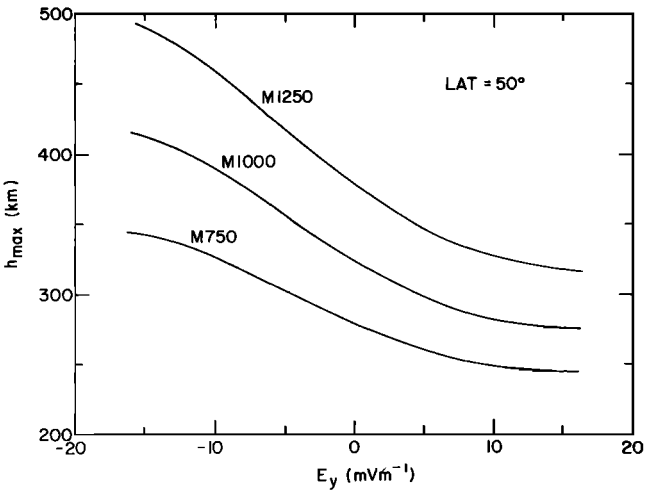

Fig. 6. Variation in the height of the F_2 layer peak density as a function of E_y for three model neutral atmospheres.

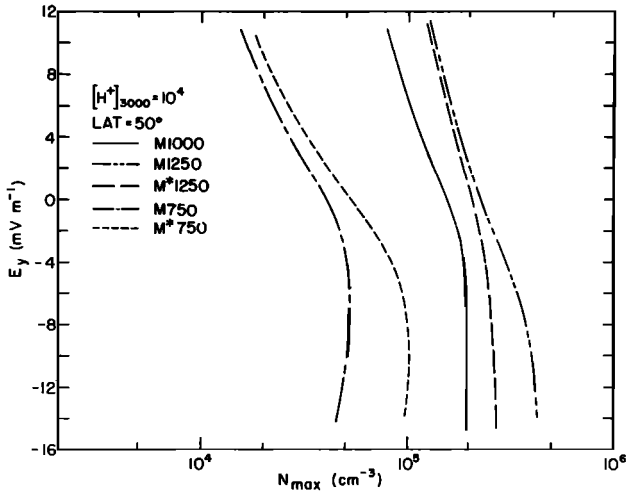

Fig. 8. The F_2 layer peak density as a function of E_y for five separate model atmospheres. Model M*750 has a smaller atomic hydrogen density than model M750, whereas the opposite is true for models M*1250 and M1250.

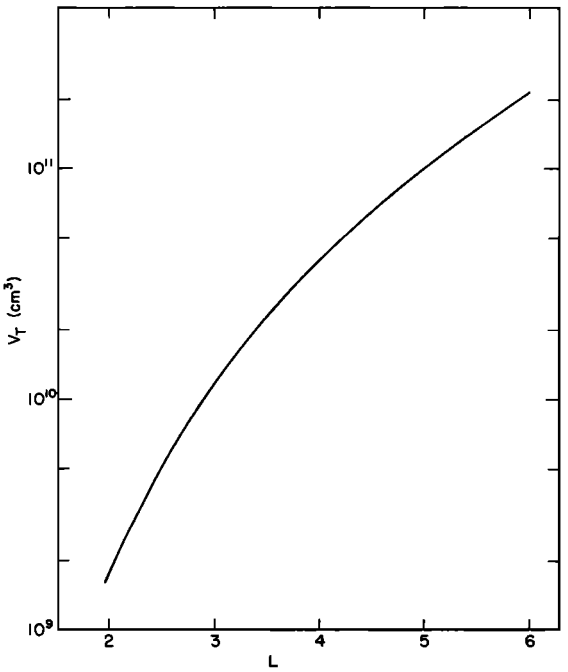

Fig. 9. Magnetic field tube volume as a function of L shell.

10*b* an equatorward neutral wind is suddenly reversed. In both figures the resulting vertical drift velocity w_D and the height of the F_2 peak density behave in about the same way. In the electric field example the plasma is initially at $L = 4$ and drifts inward to $L \simeq 3$ in about 1 hour, a decrease in field tube volume and an increase in $n_{3000}(H^+)$ consequently occurring. This collapse induces a greater flow of plasma parallel to **B** into the ionosphere and causes N_mF_2 actually to increase, even though the layer itself is being strongly pushed into regions of rapid ionization loss.

The neutral wind, in contrast, causes N_mF_2 to decrease slightly. In this case, increased plasma fluxes very nearly cancel the effect of increased losses; i.e., this situation is very similar to the steady state solutions described earlier.

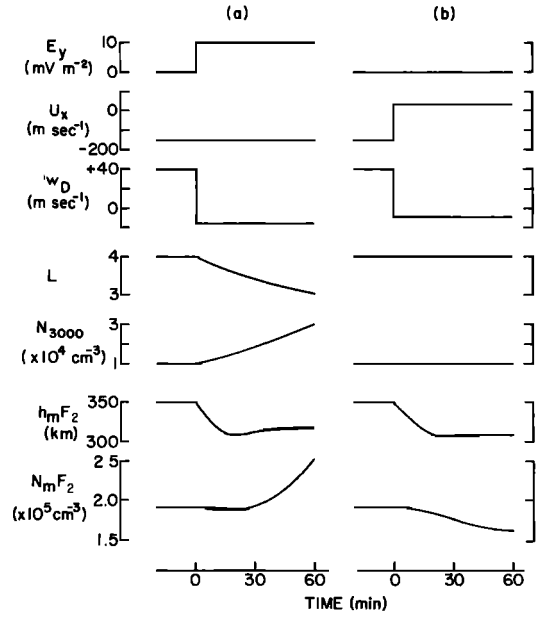

Fig. 10. Time-dependent solutions for step increases in (*a*) the westward electric field and (*b*) the southerly thermospheric wind; w_D gives the applied vertical drift velocity, L indicates the location of the flux tube, and N_{3000} gives the time-dependent value of the 3000-km H^+ density.

In both examples illustrated in Figure 10 the initial plasma content of the field tube was assumed to be 5×10^{13} ions, sufficiently large to insure that no substantial loss occurred in 1 hour. If the initial content were smaller, as might be true at low latitudes or in a period following a magnetic storm, N_mF_2 would tend to decrease more rapidly as the plasma reservoir became depleted (Figure 3).

Discussion

The present results emphasize the stability of the F_2 layer peak density to variations in external electric fields and thermospheric winds. This stability arises from the strong coupling between the F_2 region and the topside ionosphere such that downward ionization flow acts to compensate processes tending to change the peak electron (or O^+) density. The height of the layer, however, does behave in a more traditional manner. It is also emphasized that calculations of the stability of the F_2 layer densities cannot be made without coupled models of the F region and plasmasphere in which ionization fluxes are present. Such a result implies that previous computations that have relied upon a condition of diffusive equilibrium for O^+ in the topside ionosphere are subject to considerable error.

The magnitude of the peak F_2 layer density at night is seen to reflect conditions in the topside ionosphere, larger densities in the plasmasphere reservoir giving greater values of N_mF_2. Since magnetospheric substorms continually agitate the plasma density in the mid-latitude plasmasphere, a wide range of values for N_mF_2 can result. Furthermore, when the neutral hydrogen density changes as a consequence of changes in the thermospheric temperatures, there will be a direct effect upon the F_2 peak density.

The calculations of the step function response of the nighttime ionosphere-plasmasphere are particularly relevant to effects associated with magnetospheric substorms. *Park* [1971] and *Park and Meng* [1971] have reported observations of enhanced N_mF_2 in the mid-latitude winter nighttime ionosphere during substorms. These enhancements were accompanied by a lowering of the F_2 layer. The tentative explanation at that time for this behavior was given in terms of the effect of a westward electric field inducing a large influx of plasma from the plasmasphere and simultaneously lowering the height of the layer. The present results strongly support this earlier explanation.

Acknowledgments. We gratefully acknowledge many helpful comments by Henry Rishbeth and others in the course of this study. This work was supported in part through NSF grant GA-28042 at Stanford University and NASA grant NGR-05-009-075 at the University of California at San Diego. The computing facilities at Stanford University were supported in part by the National Science Foundation, Office of Computer Science, under grant GP-948.

* * *

The Editor thanks R. G. Roble and P. Stubbe for their assistance in evaluating this paper.

References

Banks, P. M., and T. E. Holzer, Features of plasma transport in the upper atmosphere, *J. Geophys. Res.*, *74*, 6304, 1969.

Banks, P. M., and G. Kockarts, *Aeronomy*, Academic, New York, 1973.

Carpenter, L. A., and S. A. Bowhill, Investigation of the physics of dynamical processes in the topside *F*-region, *Aeron. Rep. 44*, Univ. of Ill., Urbana, Sept. 1971.

Cho, H. R., and K. C. Yeh, Neutral winds and the behavior of the ionospheric F_2-region, *Radio Sci., 5,* 881, 1970.

Evans, J. V., Midlatitude *F*-region densities and temperatures at sunspot minimum, *Planet. Space Sci., 15,* 1387, 1967.

Evans, J. V., Observations of *F*-region vertical velocities at Millstone Hill, 2, Evidence for fluxes into and out of the protonosphere, *Radio Sci., 6,* 843, 1971.

Geisler, J. E., and S. A. Bowhill, An investigation of ionosphere-protonosphere coupling, *Aeron. Rep. 5,* Univ. of Ill., Urbana, 1965.

Hanson, W. B., and T. N. L. Patterson, The maintenance of the nighttime *F*-layer, *Planet. Space Sci., 12,* 979, 1964.

Kohl, H., J. W. King, and D. Eccles, An explanation of the magnetic declination effect in the ionospheric F_2-layer, *J. Atmos. Terr. Phys., 31,* 1011, 1969.

Mayr, H. G., E. G. Fontheim, and K. K. Mahajan, Effect of modified thermal conductivity on the temperature distribution in the protonosphere, *Ann. Geophys., 29,* 21, 1973.

McFarland, M., D. L. Albritton, F. C. Fehsenfeld, E. E. Ferguson, and A. L. Schmeltekopf, A flow-drift technique for ion mobility and ion-molecule reaction rate constant measurements, 2, The positive ion reactions of N^+, O^+ and N_2^+ with O_2 and O^+ with N_2 from thermal to 2 eV, *J. Chem. Phys., 59,* 6620, 1973.

Moffett, R. J., and J. A. Murphy, Coupling between the *F*-region and protonosphere: Numerical solution of the time-dependent equations, *Planet. Space Sci., 21,* 43, 1973.

Nagy, A. F., P. Bauer, and E. G. Fontheim, Nighttime cooling of the protonosphere, *J. Geophys. Res., 73,* 6259, 1968.

Park, C. G., Whistler observations of the interchange of ionization between the ionosphere and protonosphere, *J. Geophys. Res., 75,* 4249, 1970.

Park, C. G., Westward electric fields as the cause of nighttime enhancements in electron concentrations in the mid-latitude *F*-region, *J. Geophys. Res., 76,* 4560, 1971.

Park, C. G., Methods of determining electron concentrations in the magnetosphere from nose whistlers, *Tech. Rep. 3454-1,* Radio Sci. Lab., Stanford Univ., Stanford, Calif., 1972.

Park, C. G., and C.-I. Meng, Distortions of the nightside ionosphere during magnetospheric substorms, *J. Geophys. Res., 78,* 3828, 1973.

Rüster, R., The relative effects of electric fields and atmospheric composition changes on the electron concentration in the mid-latitude *F*-layer, *J. Atmos. Terr. Phys., 33,* 275, 1971.

Schunk, R. W., and J. C. G. Walker, Minor ion diffusion in the F_2-region of the ionosphere, *Planet. Space Sci., 18,* 1319, 1970.

Stubbe, P., Theory of the nighttime *F*-layer, *J. Atmos. Terr. Phys., 30,* 243, 1968.

Stubbe, P., and S. Chandra, The effect of electric fields on the *F*-region behavior as compared with neutral wind effects, *J. Atmos. Terr. Phys., 32,* 1909, 1970.

Taylor, H. A., Jr., H. C. Brinton, M. W. Pharo III, and N. K. Rahman, Thermal ions in the exosphere; Evidence of solar and geomagnetic control, *J. Geophys. Res., 73,* 5521, 1968.

Torr, D. G., and M. R. Torr, A theoretical investigation of corpuscular radiation effects on the *F*-region of the ionosphere, *J. Atmos. Terr. Phys., 32,* 15, 1970.

Yonezawa, T., Maintenance of ionization in the nighttime F_2-region, *Space Res., 5,* 49, 1965.

(Received March 25, 1974;
accepted July 17, 1974.)